

Molecular Profiling of Stroma Identifies Osteopontin as an Independent Predictor of Poor Prognosis in Intrahepatic Cholangiocarcinoma

Laurent Sulpice,^{1,2,3} Michel Rayar,^{2,3} Mireille Desille,^{1,2} Bruno Turlin,^{1,2,4} Alain Fautrel,^{1,2}
Eveline Boucher,^{1,2,5} Francisco Llamas-Gutierrez,^{2,4} Bernard Meunier,^{2,3} Karim Boudjema,^{1,2,3}
Bruno Clément,^{1,2} and Cédric Coulouarn^{1,2}

Intrahepatic cholangiocarcinoma (ICC) is the second most common type of primary cancer in the liver. ICC is an aggressive cancer with poor prognosis and limited therapeutic strategies. The identification of new drug targets and prognostic biomarkers is an important clinical challenge for ICC. The presence of an abundant stroma is a histological hallmark of ICC. Given the well-established role of the stromal compartment in the progression of cancer diseases, we hypothesized that relevant biomarkers could be identified by analyzing the stroma of ICC. By combining laser capture microdissection and gene expression profiling, we demonstrate that ICC stromal cells exhibit dramatic genomic changes. We identified a signature of 1,073 nonredundant genes that significantly discriminate the tumor stroma from nontumor fibrous tissue. Functional analysis of differentially expressed genes demonstrated that up-regulated genes in the stroma of ICC were related to cell cycle, extracellular matrix, and transforming growth factor beta (TGF β) pathways. Tissue microarray analysis using an independent cohort of 40 ICC patients validated at a protein level the increased expression of collagen 4A1/COL4A1, laminin gamma 2/LAMC2, osteopontin/SPP1, KIAA0101, and TGF β 2 genes in the stroma of ICC. Statistical analysis of clinical and pathological features demonstrated that the expression of osteopontin, TGF β 2, and laminin in the stroma of ICC was significantly correlated with overall patient survival. More important, multivariate analysis demonstrated that the stromal expression of osteopontin was an independent prognostic marker for overall and disease-free survival. *Conclusion:* The study identifies clinically relevant genomic alterations in the stroma of ICC, including candidate biomarkers for prognosis, supporting the idea that tumor stroma is an important factor for ICC onset and progression. (HEPATOLOGY 2013; 00:000-000)

Intrahepatic cholangiocarcinomas (ICC) account for 5%-10% of liver primary cancers.¹ ICC usually arise from epithelial cells of the intrahepatic small bile ducts, although a recent report in mice suggested that ICC might also originate from the conversion of mature hepatocytes.² Over the last decade, the incidence of ICC has increased significantly in Western

countries.^{3,4} This trend could be related to a better histological diagnosis of ICC and/or to the rising incidence of the main risk factors for ICC: cholangitis, chronic hepatitis B and C, diabetes, and obesity.⁵ Liver resection remains the only curative treatment for ICC but is associated with a high rate of recurrence.⁶ Recently, we showed that hilar lymph node metastasis,

Abbreviations: DFS, disease-free survival; ECM, extracellular matrix; EMT, epithelial to mesenchymal transition; FFPE, formalin-fixed paraffin-embedded; GSEA, gene set enrichment analysis; HR, hazard ratio; HCC, hepatocellular carcinoma; ICC, intrahepatic cholangiocarcinoma; IHC, immunohistochemistry; LCM, laser capture microdissection; OLT, orthotopic liver transplantation; OS, overall survival; TF, transcription factor; TGF β , transforming growth factor beta; TMA, tissue microarray.

From the ¹Inserm, UMR991, Liver Metabolisms and Cancer, Rennes, France; ²Université de Rennes 1, Rennes, France; ³CHU Rennes, Service de Chirurgie Hépatobiliaire et Digestive, Rennes, France; ⁴CHU Rennes, Service d'Anatomie et Cytologie Pathologiques, Rennes, France; ⁵Centre Régional de Lutte contre le Cancer, Rennes, France.

Received February 8, 2013; accepted June 2, 2013.

Supported by Inserm, Université de Rennes 1, Institut National du Cancer, Agence Nationale pour la Recherche and Novartis Oncology, France.

perineural invasion, and intrahepatic satellite nodules represent high risk factors for ICC recurrence in patients undergoing liver resection.⁷ For patients with nonresectable ICC, chemotherapies provide only partial benefit.^{8,9} To date, the overall prognosis of patients with ICC is poor, necessitating the identification of accurate prognostic factors and novel therapeutic strategies.

Growing evidence demonstrates that tumor onset and progression are determined not only by cancer cells themselves but also by their microenvironment.¹⁰ Microenvironment is a dynamic system which includes several types of cells (e.g., myo-fibroblasts, immune and endothelial cells), soluble factors (e.g., cytokines), and components of the extracellular matrix (ECM) which constitute the stroma of tumors. Importantly, the stroma modulates key processes of carcinogenesis, including cell communication, differentiation, invasiveness, chemoresistance, and epithelial to mesenchymal transition (EMT). Supporting the dynamic coevolution of tumor cells with their microenvironment, several studies have demonstrated that stromal gene expression signatures correlated with the progression of cancers.¹¹⁻¹³ In the liver, we have previously shown that ECM remodeling is associated with tumor progression.¹⁴ More recently, we identified a gene signature characteristic of the tumor-stroma crosstalk that was successful at predicting the survival of patients with hepatocellular carcinoma (HCC).¹⁵ We also showed that targeting the tumor-stroma crosstalk by epigenetic modulators may represent a promising therapeutic strategy in HCC.¹⁵ The presence of a dense stroma is a prominent feature of ICC, suggesting that remodeling of the tumor microenvironment may represent a key process in ICC onset and progression.¹⁶ Thus, we hypothesized that relevant prognostic biomarkers could be inferred by investigating alterations of the stroma in ICC. By laser capture microdissection (LCM), gene expression profiling, and tissue microarray analysis (TMA) we identified a gene signature of the tumor stroma in ICC from which the overexpression of osteopontin was shown to be an independent predictor of overall and disease-free survival.

Patients and Methods

Patients. A cohort of 87 patients with primary ICC was studied. These patients underwent liver resection at Rennes-University hospital between January 1997 and August 2011. Only mass-forming types of ICC were included, as defined by the Liver Cancer Study Group of Japan. Written informed consent was obtained from all patients. The study protocol fulfilled national laws and regulations and was approved by the local Ethics Committee. Freshly frozen and formalin-fixed paraffin-embedded (FFPE) tissues were provided by the biobank of the university hospital. Histological and clinical features including those observed upon follow-up examinations were obtained from hospital charts.

Laser Capture Microdissection. LCM was performed using the Arcturus Veritas Microdissection system (Applied Biosystems, Carlsbad, CA). From frozen tissues, serial sections of 10 μm were prepared using a Leica 3050 S cryostat (Leica Microsystems, Wetzlar, Germany) and mounted onto a PEN membrane glass slide (Applied Biosystems). Tissue sections were dehydrated by successive immersions (30 seconds, twice) in 70%, 90%, and 100% ethanol solutions. Enzymatic activity was locked by the immersion in a xylene solution (1 minute, twice) before performing LCM.

RNA Extraction and Gene Expression Profiling. Total RNA was purified using an Arcturus Picopure RNA isolation kit (Applied Biosystems). Genome-wide expression profiling was performed using human SurePrint G3 8x60K pangenomic microarrays (Agilent Technologies, Santa Clara, CA) as described.^{15,17} Fifty nanograms of total RNA was purified from LCM tissues and amplified with a low-input QuickAmp labeling kit (Agilent Technologies). The amplification yield was $1.8 \pm 0.7 \mu\text{g}$ complementary DNA (cRNA), and the specific activity was $5.8 \pm 3.4 \text{ pmol Cy3 per } \mu\text{g cRNA}$. Gene expression data were analyzed using Feature Extraction and GeneSpring softwares (Agilent Technologies) and further analyzed using R-based ArrayTools. Microarray data are publicly available from the gene expression omnibus (GEO) database (www.ncbi.nlm.nih.gov/geo; GSE45001). Briefly, microarray data were

Address reprint requests to: Cédric Coulouarn, Ph.D., Inserm, UMR991, Pontchaillou University Hospital, 2 rue Henri Le Guilloux, F-35033, Rennes, France.
E-mail: cedric.coulouarn@inserm.fr; fax: +33 299 540 137.

Copyright © 2013 by the American Association for the Study of Liver Diseases.

View this article online at wileyonlinelibrary.com.

DOI 10.1002/hep.26577

Potential conflict of interest: Nothing to report.

Additional Supporting Information may be found in the online version of this article.

normalized using the quantile normalization algorithm, and differentially expressed genes were identified by a two-sample univariate t test and a random variance model as described.¹⁸ Permutation P values for significant genes were computed based on 10,000 random permutations. Clustering analysis was done using Cluster 3.0 and TreeView 1.6 with uncentered correlation and average linkage options.

Data Mining and Integrative Genomics. Enrichment for specific biological functions or canonical pathways was evaluated as described.^{19,20} Gene set enrichment analysis (GSEA) was performed using the Java-tool developed at the Broad Institute (Cambridge, MA).²¹ Integration of genomic data was performed as described²² using publicly available gene expression datasets downloaded from GEO. ChIP enrichment analysis was performed using the ChEA algorithm developed by Lachmann et al.²³

Tissue Microarray (TMA). TMAs were designed with the TMA Designer software. FFPE tissues were arrayed using a Minicore 3 tissue Arrayer (Excilone, VICQ, France). After hematoxylin-eosin staining, three representative areas of stroma from each ICC tumor (T) and of fibrous tissue from portal tracts areas in the surrounding nontumor (NT) liver were selected by an experienced pathologist (B.T.). Chosen areas were punched with a cylinder of 1 mm diameter and the samples were transferred into a recipient paraffin block. Thus, each tissue block (NT and T) was represented by three independent spots in the TMA.

Immunohistochemistry (IHC). IHC experiments were performed using an automated Discovery XT immunostaining device (Ventana Medical System, Tucson, AZ). TMA sections (4 μ m thick) were evaluated for the expression of collagen 4, laminin, osteopontin, TGF β 2, and KIAA0101 (Supporting Table 1). Antigens were retrieved from deparaffinized and rehydrated tissues by incubating the slides for 48 minutes at 95°C in CC1 Tris-based buffer (pH 8.0) (laminin, collagen 4, and KIAA0101) or in Ultra CC2 citrate buffer (pH 6.0) (osteopontin and TGF β 2) (Ventana Medical System). Detection was performed using a streptavidin-biotin-peroxidase kit (OmniMap, Biotin-free DAB Detection Systems, Ventana Medical System). TMA slides were analyzed by two experienced pathologists (B.T., F.L.G.) in a blinded manner. Staining intensity in the stroma was scored as follows: negative (0), mild (1), moderate (2), or strong (3). Given that each stromal sample was represented in triplicate, the sum of the three values was performed to obtain a score of with a range of 0 to 9. This score was finally categorized into four groups to optimize the statistical analysis and to take into account

extreme values: 0 (score 0-1), 1 (score 2-3), 2 (score 4-7), and 3 (score 8-9).

Statistical Analysis. Differences in protein expression (NT fibrous tissue versus T stroma) were evaluated by chi-squared testing. Relationships between protein expression and clinical parameters were evaluated using the chi-squared or Fisher's exact probability test for categorical variables and using the analysis of variance for numerical variables. The correlation of the scoring performed by the two pathologists was estimated by a weighted kappa coefficient; disagreements were weighted according to their squared distance from a perfect agreement in the correlation matrix. The Kaplan-Meier method was used to estimate the overall (OS) and disease-free survival (DFS), and group differences were analyzed with the log-rank test. A trend analysis was also performed. Univariate and multivariate Cox regression models for the hazards of OS and DFS mortality were used to evaluate the effect of protein expression. Correlation between the different variables was also evaluated in order to identify putative interaction and confounding factors. The most suited Cox model was selected using a stepwise regression, selecting variables based on the Akaike Information Criterion (AIC). $P < 0.05$ was considered statistically significant. Statistical analysis was performed with R (v. 2.15.1).

Results

Study Design. Relevant biomarkers for ICC prognosis were investigated by the unsupervised gene expression analysis of the stroma in mass-forming type ICC. To increase the robustness of the study, an initial cohort of clinically well-annotated cases of patients with ICC ($n = 87$) was used to build a testing set and a validating set as described.²⁰ The testing set included 10 cases of freshly frozen ICC for which stroma analysis was performed by a combined approach using LCM and pangenomic microarray profiling (Supporting Table 2). Significant differences in messenger RNA (mRNA) profiles (T stroma versus matched NT fibrous tissue) were evaluated at a protein level using a validating set which consisted of 40 FFPE ICC equally distributed in cases with or without recurrence (Table 1). IHC was done using TMA to reduce experimental noise. Finally, the prognostic value of selected proteins was estimated using clinical records and patient follow-up reports (Fig. 1).

ICC Tumor Stroma Exhibits Important Genomic Changes. LCM was performed to isolate RNA from the stromal compartment of freshly frozen ICC tissues.

Table 1. Clinicopathological Features of Validating Set ICC

Clinicopathological features	n = 40
Age (years, mean \pm SD)	64.8 \pm 8.8
Gender (male:female)	30:10
Tumor size (mm, mean \pm SD)	64 \pm 29
Range	20-130
Tumor \geq 50 mm	27 (67.5%)
UICC classification, 7 th edition	
I	15 (37.5%)
II	12 (30%)
III	10 (25%)
IV	3 (7.5%)
Satellite nodules $>$ 1	8 (20%)
Positive hilar lymph nodes	9 (22.5%)
Macrovascular invasion	3 (7.5%)
Microvascular invasion	13 (32.5%)
Perineural infiltration	8 (20%)
Capsular disruption	4 (10%)
Tumoral necrosis	15 (37.5%)
Cirrhosis	9 (22.5%)
Hepatitis B/C	0 (0%)
Follow-up (months, mean \pm SD)	31.8 \pm 25.9
Range	1.5-102.4
Death	22 (55%)

For each ICC tumor, fibrous tissue from portal areas within the surrounding nontumor liver was also isolated and used as a reference (Fig. 2A). Following hybridization on microarrays, the statistical analysis focused on identifying genes for which expression was significantly altered in the stroma of ICC. As shown in Fig. 2B, applying stringent criteria ($P < 0.001$ and fold change $FC > 2$) resulted in the identification of 1,073 nonredundant genes differentially expressed between the NT fibrous tissue and the T stroma, demonstrating that the stroma of ICC displayed substantial genomic changes (Supporting Table 3). Thirty-one percent of the stromal signature included genes that were up-regulated relative to NT fibrous tissue. Supporting the gene selection, a hierarchical clustering analysis based on this signature efficiently discriminated the NT fibrous tissue from the T stroma (Fig. 2C). Fully supporting this observation, integrative genomics demonstrated that the LCM-derived stroma signature also discriminated cholangiocarcinoma tumors from surrounding NT livers in an independent genomic dataset (GSE26566) established from whole tissue sections (Fig. 2D).

Up-Regulated Genes in the Stroma Are Associated With Cell Cycling, ECM Activity, and Activation of the TGF β Pathway. Further validating the enrichment of the stromal compartment by LCM, both up- and down-regulated genes were categorized into functional modules associated with the extracellular region, including ECM (Supporting Table 4F). Down-regulated genes were enriched in gene sets known to

be down-regulated in liver cancers, including genes involved in metabolism (Supporting Table 4, Supporting Fig. 2). Up-regulated genes were related to entry into the cell cycle, ECM organization, and cell signaling pathways, namely, p38, p53, and TGF β . Accordingly, the stroma signature of ICC coincided with a discrete enrichment of transcription factor (TF)-associated gene sets (Supporting Table 4D). Indeed, up-regulated genes were known to be transcriptionally regulated by E2F(s) and SMAD(s), two families of TF involved notably in the regulation of cell cycle and TGF β signaling pathway, respectively. Down-regulated genes were regulated by hepatocyte nuclear factors known to control the expression of numerous metabolic genes (Supporting Table 4, Supporting Fig. 2). These results were confirmed by an unsupervised GSEA (Supporting Fig. 2). A significant enrichment of gene signatures representative of ECM receptor interactions, cell cycle, and TGF β signaling was also observed in the stroma of ICC (Fig. 3A-C).

Independent Set of ICC Highlights a Molecular Heterogeneity of Stromal Profiles. The expression of several genes was evaluated at a protein level in an independent set of 40 ICC (Fig. 1). Among the genes significantly up-regulated in the stroma of ICC, we focused on key genes that form our hypothesis that ECM remodeling contributes to ICC pathogenesis. Selected candidate genes were representative of the enriched functional categories identified above, including ECM components (collagen 4A1/COL4A1, laminin gamma 2/LAMC2, osteopontin/SPP1), a master gene of the TGF β pathway (TGF β 2) as well as a partially characterized gene involved in the cell cycle (KIAA0101).²⁴ The expression of these five genes was greatly increased at the RNA level in the testing set (Fig. 4A), and TMA confirmed this observation at the protein level in the validating set (Fig. 4B). Interestingly, while mRNA levels were homogeneous in the NT fibrous tissues, a greater heterogeneity of mRNA

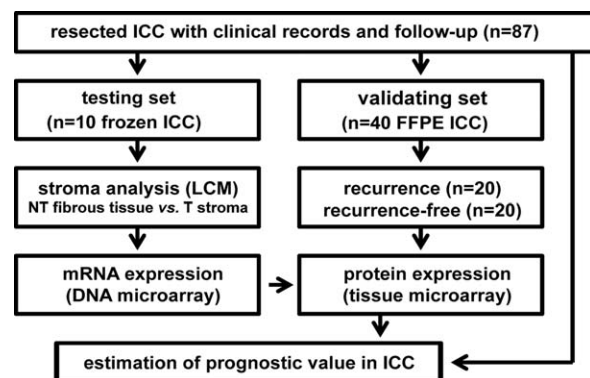


Fig. 1. Flowchart of the study design.

profiles was observed in the T stroma (Fig. 4A). Based on this observation and previously published ICC genomic profiles,²⁵⁻²⁸ we hypothesized that the variability of expression profiles of these particular genes in the stroma may reflect the heterogeneity of ICC subgroups with different prognoses.

Expression Profiles of the Tumor Stroma Are Clinically Relevant. The clinical relevance of protein expression profiles within ICC T stroma was evaluated by univariate statistical analysis. Clinical and pathological characteristics of the validating set are summarized in Table 1. Importantly, this cohort was representative of ICC cases encountered in clinical practice, particularly with an even distribution according to the International Union Against Cancer (UICC) 7th edition classification (37.5%, 30%, 25%, and 7.5% for stage

I, II, III, and IV, respectively). Analysis of the intensity of TMA staining in the stroma demonstrated statistically significant associations between laminin, osteopontin, TGF β 2, and KIAA0101 protein expression and clinical data (Table 2). Osteopontin, TGF β 2, and laminin expression in ICC T stroma was significantly correlated with patient OS. The expression of osteopontin was also significantly correlated with DFS ($P < 0.001$), tumor size ($P = 0.049$), presence of hilar lymph nodes ($P = 0.009$), and macrovascular invasion ($P = 0.04$) (Table 2, Fig. 5; Supporting Fig. 1). Importantly, the scoring of osteopontin staining was performed by two independent pathologists. The correlation between the two analyses was significant (weighted kappa coefficients were 0.831 and 0.855 for initial and categorized score, respectively), supporting osteopontin as a candidate biomarker in ICC. The overexpression of TGF β 2 was significantly associated with the UICC 7th edition classification ($P = 0.032$), microvascular invasion ($P = 0.047$), and presence of hilar lymph nodes ($P = 0.048$). In addition, KIAA0101 overexpression was correlated with perineural infiltration, which is one of the most important indicators of recurrence with the presence of hilar lymph nodes.⁷ No significant correlation was found between Collagen 4A1 staining and the clinical variables tested (Table 2).

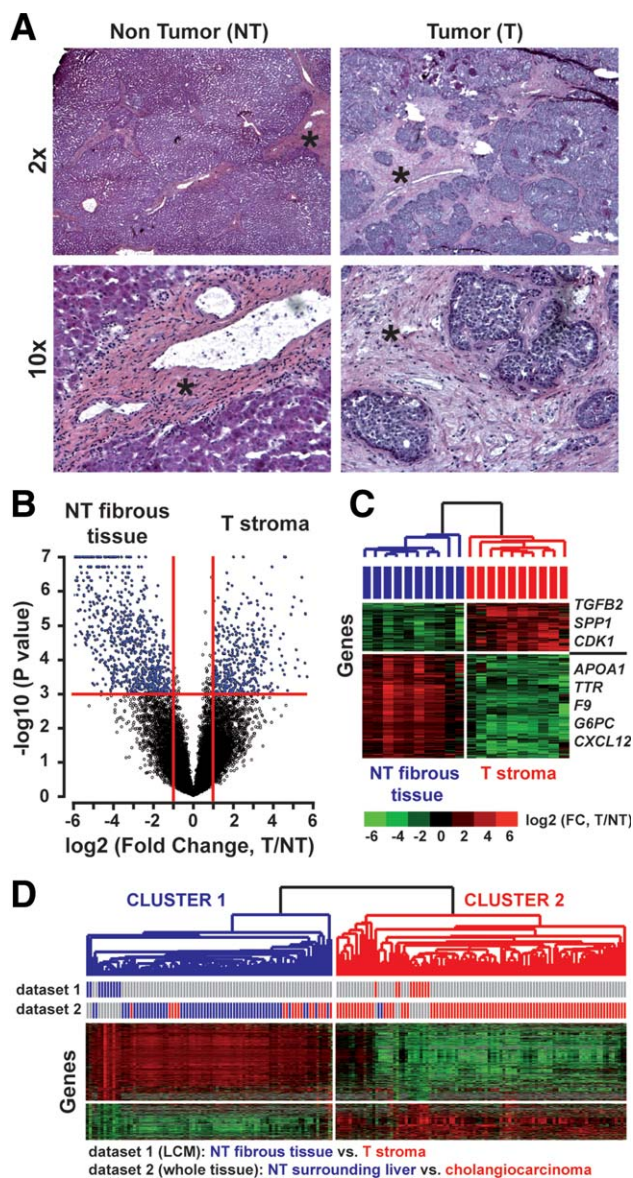


Fig. 2

Fig. 2. Gene expression profiling of microenvironment in ICC. (A) H&E staining of a representative tumor (T) tissue (right panels) and an adjacent nontumor (NT) liver tissue (left panels) from a patient with ICC. From the testing set (10 frozen ICC), laser capture microdissection (LCM) was performed to isolate RNA from NT fibrous tissue and T stroma (asterisk). Original magnification, $\times 2$ (top) and $\times 10$ (bottom). (B) Volcano plot of 1,073 nonredundant genes differentially expressed between the T stroma and the surrounding NT fibrous tissue. Following microarray analysis of the 10 frozen ICC from the testing set, genes were selected based on the significance of the differential gene expression in the T stroma versus the surrounding NT fibrous tissue (horizontal red line; $P < 0.001$) and the level of induction or repression (vertical red lines; fold-change > 2). (C) Clustering analysis of genes differentially expressed between the T stroma and the surrounding NT fibrous tissue ($n = 10$ ICC from the testing set). Examples of major changes in steady-state levels of mRNAs are indicated on the right. (D) Integrative genomic analysis of the ICC stroma gene signature using independent human gene expression profiles from patients with cholangiocarcinoma. Shown is a detailed dendrogram view of NT (blue) fibrous tissues and T (red) stroma samples obtained by LCM (dataset 1: the present study) integrated with an independent dataset of human cholangiocarcinomas (dataset 2: Andersen et al.²⁵). Dataset 2, which was uploaded from GEO (GSE26566), consisted of 104 cholangiocarcinomas (T, red) and 59 nontumoral surrounding liver tissues (NT, blue). Validating the stroma signature in an independent cohort of patients, the clustering analysis of tissue samples based on the expression of 1,073 genes differentially expressed between the NT fibrous tissue and the T stroma identified two main clusters which respectively included the NT fibrous tissue and most of the NT human tissues (cluster 1), and the T stroma and most of the cholangiocarcinomas (cluster 2).

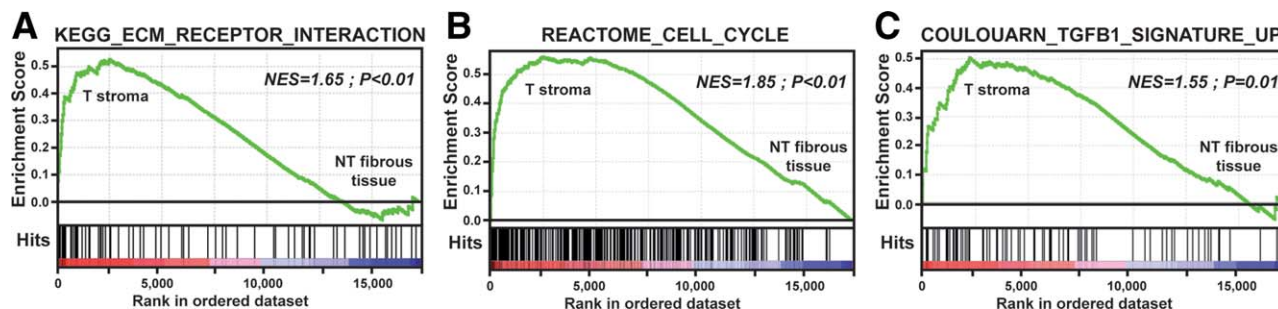


Fig. 3. Functional analysis of the ICC stroma signature. (A-C) Gene set enrichment analysis (GSEA) using the gene expression profiles of ICC T stroma (left side) and adjacent NT fibrous tissue (right side). GSEA demonstrated a significant enrichment of gene signatures associated with ECM (A), cell cycle (B), and TGF β pathway (C), specifically in the gene profiles of ICC T stroma ($P < 0.01$). NES, normalized enrichment score from GSEA algorithm.

Stromal Expression of Osteopontin Is an Independent Factor of Prognosis. Univariate and multivariate analyses of risk factors influencing OS and DFS were performed (Table 3). Among 14 factors assessed by the univariate analysis, the number of nodules ($P = 0.027$), capsular disruption ($P = 0.030$), TGF $\beta 2$ staining ($P < 0.001$), and osteopontin staining ($P < 0.001$) were significantly associated with OS.

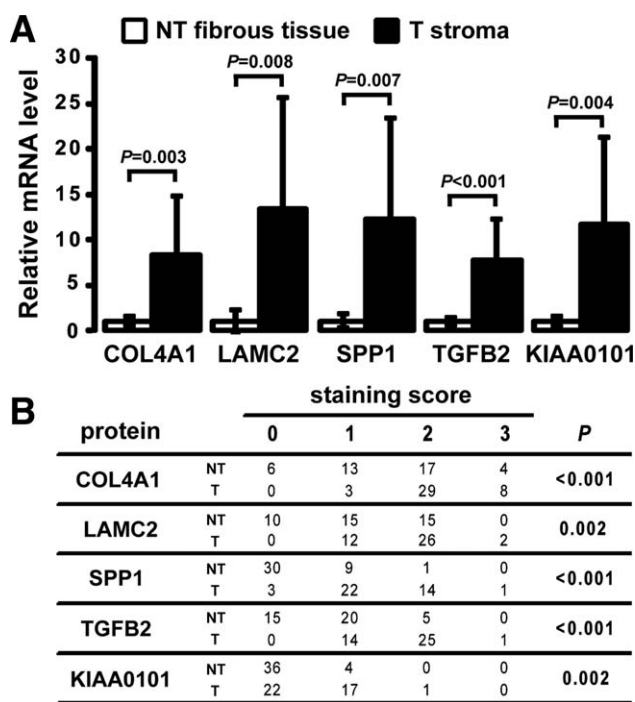


Fig. 4. Validation of mRNA profiles at a protein level. (A) mRNA analysis of selected genes demonstrated a significant increase in the expression of COL4A1, LAMC2, SPP1 (osteopontin), TGF $\beta 2$, and KIAA011 in the stroma of ICC compared to the adjacent NT fibrous tissue. Normalized microarray values are shown. The P -value was determined by using a two-tailed Student t test. (B) Immunohistological analysis of COL4A1, LAMC2, SPP1, TGF $\beta 2$, and KIAA011 protein expression in the T stroma (T) and the surrounding NT fibrous tissue (NT) of an independent set of 40 patients with ICC. Staining was scored as described in the Patients and Methods section: negative (0), mild (1), moderate (2), or strong (3). The expression of all proteins was significantly increased in the stroma of ICC.

Analysis of correlation between the different variables did not show any potential confounding interactions, as no values were above 0.7 (Supporting Table 5). By multivariate analysis, the number of nodules (hazard ratio [HR], 2.0; 95% confidence interval [CI], 1.3-3.2; $P = 0.002$), capsular disruption (HR, 6.4; 95% CI, 1.5-27.4; $P = 0.012$), and osteopontin staining (HR, 3.2; CI 95%, 1.3-7.5; $P = 0.009$) were identified as independent risk factors for reduced OS. Independent risk factors for reduced DFS included number of nodules (HR, 2; 95% CI, 1.4-3; $P < 0.001$), positive hilar lymph node (HR, 3; 95% CI, 1-8.8; $P = 0.048$), capsular disruption (HR, 5.8; 95% CI, 1.6-20.3; $P = 0.006$), and osteopontin staining (HR, 2.5; 95% CI, 1.1-6; $P < 0.001$). Altogether, these results highlighted the stromal overexpression of osteopontin as an independent factor of poor prognosis in ICC.

Discussion

In the present study we established the genomic profiles of the stromal compartment of ICCs and investigated their clinical relevance. Combining LCM and gene expression profiling, the expression of 1,073 genes was found to significantly discriminate the

Table 2. Statistical Analysis of Protein Expression in View of Clinical and Pathological Features of ICC Patients

Variables	COL4A1	LAMC2	OSTEOP.	TGF $\beta 2$	KIAA0101
UICC classification, 7 th Ed.	ns	ns	ns	0.032	ns
Tumor size	ns	ns	0.049 *	ns	ns
Satellite nodules >1	ns	ns	ns	ns	ns
Microvascular invasion	ns	ns	ns	0.047	ns
Positive hilar lymph nodes	ns	ns	0.009	0.048	ns
Perineural infiltration	ns	ns	ns	ns	0.043
Macrovascular invasion	ns	ns	0.040	ns	ns
Capsular disruption	ns	ns	ns	ns	ns
Tumoral necrosis	ns	ns	ns	ns	ns
OS	ns	0.018	<0.001	<0.001	ns
DFS	ns	ns	<0.001	ns	ns

* P value as determined in the Methods section.

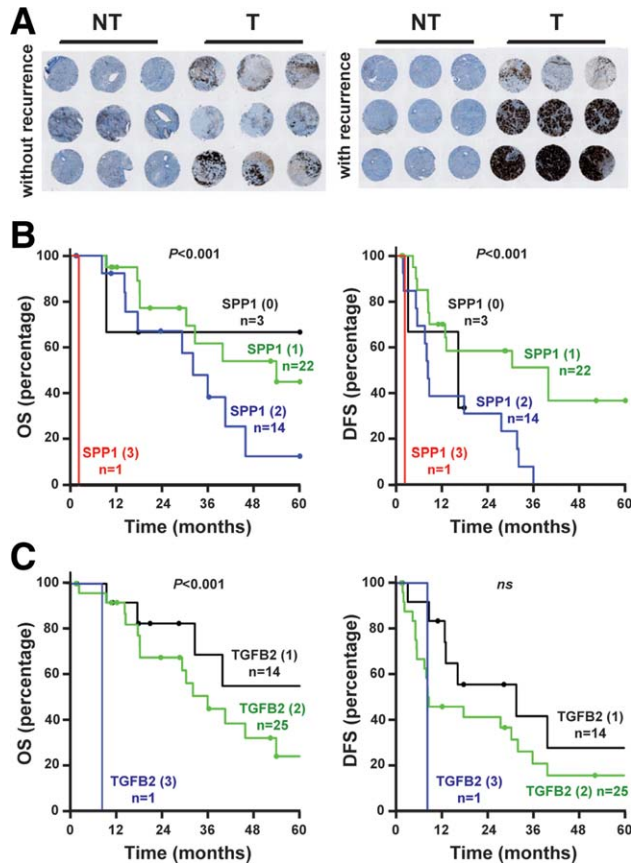


Fig. 5. Stromal overexpression of osteopontin and TGFβ2 correlates with a poor prognosis in patients with ICC. (A) Representative immunohistological analysis of osteopontin expression by tissue microarray in patients with or without recurrence (right and left panels, respectively). NT, nontumoral tissue; T, tumoral tissue. (B,C) Kaplan-Meier curves and log-rank analysis of overall survival (OS) (left panels) and disease-free survival (DFS) (right panels) according to the expression of SPP1/osteopontin (B) or TGFβ2 (C) in the stroma of ICC. Staining was scored as negative (0), mild (1), moderate (2), or strong (3).

tumor stroma from the nontumoral fibrous tissue of portal areas. Among up-regulated genes, we validated the dysregulation of osteopontin at the protein level in an independent cohort of 40 ICC, and we demonstrated that the overexpression of osteopontin in the stroma of ICC was an independent risk factor for OS and DFS.

Changes in the crosstalk between cancer cells and their microenvironment is a well-recognized hallmark of cancer progression. The clinical relevance of genomic alterations of stromal cells has been reported in several solid tumors such as breast and lung carcinomas.²⁹⁻³¹ In liver cancers, tumor onset and formation are associated with important stromal changes, including fibrosis/cirrhosis and ECM remodeling.¹⁴ Recently, Budhu et al.³² reported at a genomic level the prognostic value of a gene signature associated with the tumor microenvironment in HCC. Similarly, a five-

gene signature from tumor stroma predicted HCC prognosis.³³ Recently, we also reported a gene signature specific of the crosstalk between hepatocytes and activated stellate cells from the tumor microenvironment. Importantly, this signature was predictive of a poor prognosis and metastatic propensity in HCC.¹⁵ Altogether, these results strongly suggest that the tumor stroma may represent a relevant target for identifying biomarkers for cancer prognosis. Stroma is an important histological hallmark of ICC, suggesting that it may greatly influence tumor progression. However, few studies have specifically investigated the alterations of the stroma in ICC, particularly at a genomic scale. Notably, a genome-wide comparative analysis of tumor epithelia and stroma from 23 cholangiocarcinomas was recently reported.²⁵ Tumor epithelium was characterized by the dysregulation of the HER2 network and frequent overexpression of EGFR, whereas the stroma was enriched in inflammatory cytokines.²⁵

Table 3. Univariate and Multivariate Analysis of Factors Associated With Overall (A) and Disease-Free (B) Survival

Variables	Univariate (Log-Rank Test)	Multivariate (Cox Model)	
	P Value	P Value	Hazard Ratio [95% CI]
(A)			
Gender	0.225	—	
Age (years) *	0.595	—	
Tumor size†	0.183	—	
AJCC classification	0.363	—	
Number of nodules	0.027	0.002	20.017 [1.287; 3.160]
Microvascular invasion	0.248	—	
Perineural infiltration	0.071	—	
Positive lymph node	0.630	—	
Macrovascular invasion	0.372	—	
Capsular disruption	0.030	0.012	6.400 [1.496; 27.381]
Tumoral necrosis	0.976	—	
Cirrhosis	0.901	—	
TGFβ2 staining	<0.001	—	
Osteopontin staining	<0.001	0.009	3.156 [1.327; 7.504]
(B)			
Gender	0.694	—	
Age*	0.484	—	
Tumor size†	0.047	—	
AJCC classification	0.002	—	
Number of nodules	<0.001	< 0.001	20.047 [1.384; 30.025]
Microvascular invasion	0.066	—	
Perineural infiltration	0.006	—	
Positive lymph node	0.018	0.048	2.977 [10.008; 8.791]
Macrovascular invasion	0.098	—	
Capsular disruption	0.030	0.006	5.776 [1.646; 20.269]
Tumoral necrosis	0.541	—	
Cirrhosis	0.875	—	
TGFβ2 staining	0.264	—	
Osteopontin staining	<0.001	0.035	2.538 [10.068; 60.028]

*Age was defined as <65 years or ≥65 years.

†Tumor size was defined as <50 mm or ≥50 mm.

This study provided not only an important insight into the pathogenesis of cholangiocarcinoma but also novel therapeutic targets. However, these studies were not designed to investigate the molecular heterogeneity of the stroma or to define specific gene dysregulations in the stromal compartment of ICC. Herein, we specifically addressed these issues by performing gene expression profiling of microdissected stroma from human ICC. Also, while previous studies analyzed several types of cholangiocarcinomas with different prognoses (e.g., peri-hilar, infiltrating, and mass-forming type), our study exclusively focused on the mass-forming type of ICC. The robustness of the results was evaluated using two independent cohorts of patients with ICC. Importantly, the cases included representatives of all groups of ICC, as defined by the staging system of the UICC classification (Table 1; Supporting Table 2). The validating set was also equally distributed in cases with or without recurrence. Thus, although the cohort is small, we believe that the cases are likely representative of ICC. A good agreement was found for all genes evaluated at the mRNA level in the testing set and at the protein level in the validating set. Univariate and multivariate statistical analysis of protein expression and clinical features demonstrated that an overexpression of osteopontin in the stroma was closely associated with a poor prognosis in ICC. Osteopontin is a multifunctional secreted glycoprotein also known as the secreted phosphoprotein 1 (SPP1), which interacts with CD44 and integrins. Although initially discovered in bone tissue,³⁴ osteopontin is equally present in the liver, especially in the epithelium of the bile ducts and in stellate and Kupffer cells.³⁵ Osteopontin plays a pivotal role in mediating tumor-stroma interactions and in modulating cell adhesion, tissue remodeling, and tumor invasiveness, as previously described in colon and liver cancers.³⁶⁻³⁹ In HCC, several studies have demonstrated that osteopontin blockade resulted in the inhibition of tumor growth, migration, and invasion, both *in vitro* and *in vivo*.^{40,41} Besides a functional role in cancer, osteopontin also exhibits great potential as a diagnostic and/or prognostic biomarker. Indeed, the plasma level of osteopontin was shown to correlate with poor prognosis in several cancers, including HCC.⁴²⁻⁴⁵ In ICC, while osteopontin was identified as one of the most overexpressed genes,⁴⁶ to date no study correlated its expression in the stroma with aggressiveness. We also identified TGF β 2 as a good candidate biomarker for ICC prognosis. Importantly, osteopontin and TGF β 2 protein expression were the most correlated independent variables (Supporting Table 5). Accordingly, differences in OS ($P = 0.06$) and DFS ($P = 0.008$) could be also observed by combining

the expression of TGF β 2 and osteopontin (Supporting Fig. 3).

Identifying ICC with favorable or unfavorable prognoses might orientate the selection of the most appropriate treatment, including liver resection/transplantation, chemotherapy, and targeted therapy, either alone or in combination. Although ICC is not currently a widely accepted indication for orthotopic liver transplantation (OLT), some studies suggest that OLT could be indicated for selected ICC patients, as suggested for hilar cholangiocarcinoma.⁴⁷ A combination of neoadjuvant therapy followed by OLT in appropriately selected patients with unresectable ICC also demonstrated promising disease recurrence-free survival.⁴⁸ Given that the expression of osteopontin correlates with relevant clinical variables (OS, DFS, hilar lymph nodes, macrovascular invasion), we believe that patients with low to absent expression may benefit from OLT.

In conclusion, by using an unsupervised approach we showed a clear correlation between genomic changes in the stroma and the aggressiveness of ICC, and we identified osteopontin as a promising prognostic biomarker. In addition, these observations support the idea that targeting the tumor stroma may represent a valid and innovative therapeutic strategy in ICC.

Acknowledgment: The authors thank the Plateforme Génomique Santé, the Centre de Ressources Biologiques Santé (Rennes), the Liver Biobanks Network, and Pascale Bellaud from the H2P2 histopathological platform (Biosit, Rennes). C.C. thanks Dr. Wendy T. Watford from the University of Georgia for critically reviewing the article.

References

- Jemal A, Bray F, Center MM, Ferlay J, Ward E, Forman D. Global cancer statistics. *CA Cancer J Clin* 2011;61:69-90.
- Fan B, Malato Y, Calvisi DF, Naqvi S, Razumilava N, Ribback S, et al. Cholangiocarcinomas can originate from hepatocytes in mice. *J Clin Invest* 2012;122:2911-2915.
- Patel T. Increasing incidence and mortality of primary intrahepatic cholangiocarcinoma in the United States. *HEPATOLOGY* 2001;33:1353-1357.
- Yang JD, Kim B, Sanderson SO, Sauver JS, Yawn BP, Larson JJ, et al. Biliary tract cancers in Olmsted County, Minnesota, 1976-2008. *Am J Gastroenterol* 2012;107:1256-1262.
- Chaiterakij R, Yang JD, Harmsen WS, Slettedahl SW, Mettler TA, Fredericksen ZS, et al. Risk factors for intrahepatic cholangiocarcinoma: association between metformin use and reduced cancer risk. *HEPATOLOGY* 2013;57:648-655.
- Cho SY, Park SJ, Kim SH, Han SS, Kim YK, Lee KW, et al. Survival analysis of intrahepatic cholangiocarcinoma after resection. *Ann Surg Oncol* 2010;17:1823-1830.
- Sulpice L, Rayar M, Boucher E, Pracht M, Meunier B, Boudjema K. Treatment of recurrent intrahepatic cholangiocarcinoma. *Br J Surg* 2012;99:1711-1717.
- Feisthammel J, Schoppmeyer K, Mossner J, Schulze M, Caca K, Wiedmann M. Irinotecan with 5-FU/FA in advanced biliary tract

- adenocarcinomas: a multicenter phase II trial. *Am J Clin Oncol* 2007; 30:319-324.
9. Lee GW, Kang JH, Kim HG, Lee JS, Lee JS, Jang JS. Combination chemotherapy with gemcitabine and cisplatin as first-line treatment for immunohistochemically proven cholangiocarcinoma. *Am J Clin Oncol* 2006;29:127-131.
 10. Hanahan D, Weinberg RA. Hallmarks of cancer: the next generation. *Cell* 2011;144:646-674.
 11. Fukino K, Shen L, Patocs A, Mutter GL, Eng C. Genomic instability within tumor stroma and clinicopathological characteristics of sporadic primary invasive breast carcinoma. *JAMA* 2007;297:2103-2111.
 12. Kalluri R, Zeisberg M. Fibroblasts in cancer. *Nat Rev Cancer* 2006;6: 392-401.
 13. Sund M, Kalluri R. Tumor stroma derived biomarkers in cancer. *Cancer Metastasis Rev* 2009;28:177-183.
 14. Theret N, Musso O, Turlin B, Lotrian D, Bioulac-Sage P, Campion JP, et al. Increased extracellular matrix remodeling is associated with tumor progression in human hepatocellular carcinomas. *HEPATOLOGY* 2001;34:82-88.
 15. Coulouarn C, Corlu A, Glaise D, Guenon I, Thorgeirsson SS, Clement B. Hepatocyte-stellate cell cross-talk in the liver engenders a permissive inflammatory microenvironment that drives progression in hepatocellular carcinoma. *Cancer Res* 2012;72:2533-2542.
 16. Sirica AE. The role of cancer-associated myofibroblasts in intrahepatic cholangiocarcinoma. *Nat Rev Gastroenterol Hepatol* 2012;9:44-54.
 17. Lavergne E, Hendaoui I, Coulouarn C, Ribault C, Leseur J, Eliat PA, et al. Blocking Wnt signaling by SFRP-like molecules inhibits in vivo cell proliferation and tumor growth in cells carrying active beta-catenin. *Oncogene* 2011;30:423-433.
 18. Coulouarn C, Gomez-Quiroz LE, Lee JS, Kaposi-Novak P, Conner EA, Goldina TA, et al. Oncogene-specific gene expression signatures at preneoplastic stage in mice define distinct mechanisms of hepatocarcinogenesis. *HEPATOLOGY* 2006;44:1003-1011.
 19. Berriz GF, Beaver JE, Cenik C, Tasan M, Roth FP. Next generation software for functional trend analysis. *Bioinformatics* 2009;25:3043-3044.
 20. Coulouarn C, Cavard C, Rubbia-Brandt L, Audebourg A, Dumont F, Jacques S, et al. Combined hepatocellular-cholangiocarcinomas exhibit progenitor features and activation of Wnt and TGFbeta signaling pathways. *Carcinogenesis* 2012;33:1791-1796.
 21. Coulouarn C, Factor VM, Andersen JB, Durkin ME, Thorgeirsson SS. Loss of miR-122 expression in liver cancer correlates with suppression of the hepatic phenotype and gain of metastatic properties. *Oncogene* 2009;28:3526-3536.
 22. Coulouarn C, Factor VM, Thorgeirsson SS. Transforming growth factor-beta gene expression signature in mouse hepatocytes predicts clinical outcome in human cancer. *HEPATOLOGY* 2008;47:2059-2067.
 23. Lachmann A, Xu H, Krishnan J, Berger SI, Mazloom AR, Ma'ayan A. ChEA: transcription factor regulation inferred from integrating genome-wide ChIP-X experiments. *Bioinformatics* 2010;26:2438-2444.
 24. Liu L, Chen X, Xie S, Zhang C, Qiu Z, Zhu F. Variant 1 of KIAA0101, overexpressed in hepatocellular carcinoma, prevents doxorubicin-induced apoptosis by inhibiting p53 activation. *HEPATOLOGY* 2012;56:1760-1769.
 25. Andersen JB, Spee B, Blechacz BR, Avital I, Komuta M, Barbour A, et al. Genomic and genetic characterization of cholangiocarcinoma identifies therapeutic targets for tyrosine kinase inhibitors. *Gastroenterology* 2012;142:1021-1031 e1015.
 26. Obama K, Ura K, Li M, Katagiri T, Tsunoda T, Nomura A, et al. Genome-wide analysis of gene expression in human intrahepatic cholangiocarcinoma. *HEPATOLOGY* 2005;41:1339-1348.
 27. Oishi N, Kumar MR, Roessler S, Ji J, Forgues M, Budhu A, et al. Transcriptomic profiling reveals hepatic stem-like gene signatures and interplay of miR-200c and epithelial-mesenchymal transition in intrahepatic cholangiocarcinoma. *HEPATOLOGY* 2012;56:1792-1803.
 28. Sia D, Hoshida Y, Villanueva A, Roayaie S, Ferrer J, Tabak B, et al. Integrative molecular analysis of intrahepatic cholangiocarcinoma reveals 2 classes that have different outcomes. *Gastroenterology* 2013; 144:829-840.
 29. Finak G, Bertos N, Pepin F, Sadekova S, Souleimanova M, Zhao H, et al. Stromal gene expression predicts clinical outcome in breast cancer. *Nat Med* 2008;14:518-527.
 30. Karnoub AE, Dash AB, Vo AP, Sullivan A, Brooks MW, Bell GW, et al. Mesenchymal stem cells within tumour stroma promote breast cancer metastasis. *Nature* 2007;449:557-563.
 31. Meng H, Chen G, Zhang X, Wang Z, Thomas DG, Giordano TJ, et al. Stromal LRP1 in lung adenocarcinoma predicts clinical outcome. *Clin Cancer Res* 2011;17:2426-2433.
 32. Budhu A, Forgues M, Ye QH, Jia HL, He P, Zanetti KA, et al. Prediction of venous metastases, recurrence, and prognosis in hepatocellular carcinoma based on a unique immune response signature of the liver microenvironment. *Cancer Cell* 2006;10:99-111.
 33. Gao Q, Wang XY, Qiu SJ, Zhou J, Shi YH, Zhang BH, et al. Tumor stroma reaction-related gene signature predicts clinical outcome in human hepatocellular carcinoma. *Cancer Sci* 2011;102:1522-1531.
 34. Prince CW, Oosawa T, Butler WT, Tomana M, Bhowan AS, Bhowan M, et al. Isolation, characterization, and biosynthesis of a phosphorylated glycoprotein from rat bone. *J Biol Chem* 1987;262:2900-2907.
 35. Gotoh M, Sakamoto M, Kanetaka K, Chuuma M, Hirohashi S. Overexpression of osteopontin in hepatocellular carcinoma. *Pathol Int* 2002;52: 19-24.
 36. Agrawal D, Chen T, Irby R, Quackenbush J, Chambers AF, Szabo M, et al. Osteopontin identified as lead marker of colon cancer progression, using pooled sample expression profiling. *J Natl Cancer Inst* 2002;94:513-521.
 37. Bhattacharya SD, Mi Z, Kim VM, Guo H, Talbot LJ, Kuo PC. Osteopontin regulates epithelial mesenchymal transition-associated growth of hepatocellular cancer in a mouse xenograft model. *Ann Surg* 2012;255: 319-325.
 38. Pan HW, Ou YH, Peng SY, Liu SH, Lai PL, Lee PH, et al. Overexpression of osteopontin is associated with intrahepatic metastasis, early recurrence, and poorer prognosis of surgically resected hepatocellular carcinoma. *Cancer* 2003;98:119-127.
 39. Rohde F, Rimkus C, Friederichs J, Rosenberg R, Marthen C, Doll D, et al. Expression of osteopontin, a target gene of de-regulated Wnt signaling, predicts survival in colon cancer. *Int J Cancer* 2007;121:1717-1723.
 40. Sun BS, Dong QZ, Ye QH, Sun HJ, Jia HL, Zhu XQ, et al. Lentiviral-mediated miRNA against osteopontin suppresses tumor growth and metastasis of human hepatocellular carcinoma. *HEPATOLOGY* 2008;48:1834-1842.
 41. Zhao J, Dong L, Lu B, Wu G, Xu D, Chen J, et al. Down-regulation of osteopontin suppresses growth and metastasis of hepatocellular carcinoma via induction of apoptosis. *Gastroenterology* 2008;135:956-968.
 42. Cao DX, Li ZJ, Jiang XO, Lum YL, Khin E, Lee NP, et al. Osteopontin as potential biomarker and therapeutic target in gastric and liver cancers. *World J Gastroenterol* 2012;18:3923-3930.
 43. Shang S, Plymoth A, Ge S, Feng Z, Rosen HR, Sangrajang S, et al. Identification of osteopontin as a novel marker for early hepatocellular carcinoma. *HEPATOLOGY* 2012;55:483-490.
 44. Zhang CH, Xu GL, Jia WD, Ge YS, Li JS, Ma JL, et al. Prognostic significance of osteopontin in hepatocellular carcinoma: a meta-analysis. *Int J Cancer* 2012;130:2685-2692.
 45. Zhou C, Zhou HJ, Zhang XF, Lou LL, Ye QH, Zheng Y, et al. Postoperative serum osteopontin level is a novel monitor for treatment response and tumor recurrence after resection of hepatitisB-related hepatocellular carcinoma. *Ann Surg Oncol* 2013;20:929-937.
 46. Hass HG, Nehls O, Jobst J, Frilling A, Vogel U, Kaiser S. Identification of osteopontin as the most consistently over-expressed gene in intrahepatic cholangiocarcinoma: detection by oligonucleotide microarray and real-time PCR analysis. *World J Gastroenterol* 2008;14:2501-2510.
 47. Fu BS, Zhang T, Li H, Yi SH, Wang GS, Xu C, et al. The role of liver transplantation for intrahepatic cholangiocarcinoma: a single-center experience. *Eur Surg Res* 2011;47:218-221.
 48. Rana A, Hong JC. Orthotopic liver transplantation in combination with neoadjuvant therapy: a new paradigm in the treatment of unresectable intrahepatic cholangiocarcinoma. *Curr Opin Gastroenterol* 2012;28:258-265.